Joint Trajectory-Task-Cache Optimization with Phase-Shift Design of RIS-Assisted UAV for MEC

Haibo Mei, Kun Yang, *IEEE Senior Member*, Jun Shen, Qiang Liu, *IEEE Member*

***Abstract*—Unmanned aerial vehicle (UAV) can work as mobile edge computing (MEC) server in the sky to provide communication and computation services to ground terminals (GTs), due to its high mobility. However, UAV might work in complicated environment, where UAV-GT links being frequently blocked by ground obstacles, then leading to a poor quality of service (QoS) on task latency. To this problem, reconfigurable intelligent surface (RIS) can assist UAV and improve the wireless environment by reflecting the transmitted signals between the UAV and GTs. RIS-assisted UAV thus can have a greatly improved performance on mobile computing. Under this deployment, to maximize the energy-efficiency of the RIS-assisted UAV, this letter tries to study the joint optimization of UAV trajectory, task offloading and cache with the phase-shift design of the RIS. We intent to ultilize the successive convex approximation (SCA) method to solve the joint problem, which is non-convex in its original form. Numerical results show that the joint optimization can improve the performance of the RIS-assisted UAV, compared with the benchmark solutions.**

Intex Terms - Reconfigurable Intelligent Surface (RIS), Mobile Edge Computing (MEC), Task Offloading and Cache, 3D-Trajectory, Unmanned Aerial Vehicle (UAV)

I. Introduction

NOWADAYS, unmanned aerial vehicle (UAV) becomes popular to work as mobile edge computing (MEC) server [1] to provide communication and computation services to ground terminals (GTs). Numbers of works have tried to enable the energy-efficiency performance of the UAV to have prolonged mission time [2], and jointly optimize the behaviours of UAV and GTs to improve the quality of service (QoS) of GT tasks on latency [3]. For example, the authors of [4] jointly optimized the UAV trajectory and communication resource allocation to reach the maximized sum-data-rate of the system. Then GTs can easily offload its task data to the UAV and receive the results. The work in [5] proposed the solution to jointly optimize the UAV trajectory and task offloading strategies, to control the UAV flying an energy-efficient route with GTs either offloading their tasks to the UAV or processing them locally in a dynamic manner. The work in [6] further deployed cache mechanism into UAV to save the data transmission between UAV and GT. Afterwards, a method jointly solving the trajectory-task-cache problem of the MEC-enabled UAV has been provided in [7].

{Haibo Mei, Kun Yang, Qiang Liu} are with the School of Communication and Information Engineering, University of Electronic Science and Technology of China. E-mail: {haibo.mei,kunyang,liuqiang}@uestc.edu.cn.

Jun Shen is with the Yangtze Delta Region Institute (Quzhou), University of Electronic Science and Technology of China, Quzhou, China. E-mail: gxglshenjun@sina.com.

Kun Yang is also with School of Computer Technology and Engineering, Changchun Institute of Technology, Changchun, China.

Most of the above works however only considered the UAV working in a wireless environment with perfect line of sight (LoS) link to GTs, which is not the real situation. In most cases, like urban area, the UAV-GT connections might be frequently blocked by the ground obstacles like buildings, due to the high mobility of the UAV, and lead to a longer task latency of each GT task. To this problem, reconfigurable intelligent surface (RIS) has recently emerged as a promising technology to intensively improve the propagation environment in various wireless networks [8]. A RIS is a meta-surface equipped with integrated electronic circuits that can be programmed to alter an incoming electromagnetic field in a customizable way [9]. RIS therefore can easily reflect the incident signals between the sender and receiver to realize LoS connection [10].

To this new technology, RIS-assisted UAV has been recently proposed, where RIS either deployed on the surface of buildings to redirect the signals between UAV and GT [10], or on the UAV to redirect the signals between base stations and GT [11]. The works in [10] [12] jointly optimized the UAV trajectory and RIS passive bean-forming to maximize the data transmission rate. Nevertheless, there is no work intensively studying RIS-assisted UAV that works as the MEC server yet.

Here, considering RIS-assisted UAV working as MEC server, we utilize successive convex approximation (SCA) to solve the joint problem of the UAV on trajectory design, task offloading and cache, which is non-convex in its original form. The optimizaiton also considers the design of the phase-shift of the RIS, by which all the elements of the RIS can be jointly adjusted according to the timely locations of the UAV and GTs to reach the alignment of different signals. With the proposed solution, the RIS-assisted UAV will have high energy-efficiency and improved QoS of GT tasks on latency.

II. System Model and Problem Formulation

A. System Model

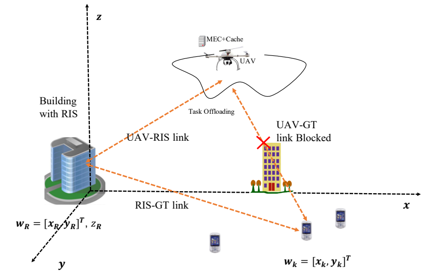

Fig. 1. RIS-assisted UAV working as the MEC server

1) Assumptions on UAV and GTs: In Fig.1, one rotary-wing UAV is deployed to work as a MEC server and equipped with cache to serve GTs in the field, and there are $\mathcal{K} \triangleq \{1, 2, ..., K\}$ static GTs on the ground with $w_k = [x_k, y_k]^T \in \mathbb{R}^{2\times1}, \forall k$ being the locations. In this letter, we will not consider fixed-wing UAV, as it cannot hover statically in the air to establish stable UAV-GT links. We assume that the UAV and GTs are equipped with a single omni-directional antenna [10], and UAV-GT link works in half-duplex mode. One k-th GT has an expected computing task $U_k = \{F_k, D_k, T_k\}$, where F_k describes the total number of the CPU cycles to be computed; D_k denotes the amount of input data to be transferred through the uplink; T_k denotes the task's completion deadline.

We discretize the UAV path into N line segments, which are represented by $N+1$ waypoints in 2D coordinates: $\{q_n\}_{n=1}^{N+1}$, where $q_n = \{x_n, y_n\}$ is the horizontal coordinate of the UAV at the n-th waypoint. We assume the UAV flying a trajectory with fixed height H. Further, one has $q_1 = q_{N+1}$ to indicate UAV flying back to its initial location in each mission. To simplify the analysis, we impose: $\|q_{n+1} - q_n\| \leq \Delta^h_{\text{max}}, n = 1, ..., N$, to constraint UAV flying with constant horizontal velocity. Furthermore, the UAV mission completion time is given by $T_u = \sum_{n=1}^{N} t_n$, where $\{t_n\}_{n=1}^{N}$ representing the time that the UAV spends within each line segment. Note that with the given maximum UAV horizontal speed V^h_{max}, the number of time slots N can be chosen sufficiently large, such that the UAV's location change within each time slot t_n can be assumed to be negligible as compared to the link distances from the UAV to GTs.

Based on the path discretization, the horizontal flying velocity of the UAV along the n-th line segment can be denoted as $0 \leq v^h_n = \frac{\sqrt{\|q_{n+1}-q_n\|^2}}{t_n} \leq V^h_{\text{max}}, n = 1, ..., N$. With the velocity, the propulsion energy of the rotary-wing UAV at each time slot can be denoted as [*].

$$e^{\text{uav}}_n = t_n \Bigg(P_0 (1 + \frac{3(v^h_n)^2}{U^2_{\text{tip}}}) + \frac{1}{2} d_0 \rho s G (v^h_n)^3 + P_1 \left(\sqrt{1 + \frac{(v^h_n)^4}{4v_0^4}} - \frac{(v^h_n)^2}{2v_0^2} \right)^{\frac{1}{2}} \Bigg) \tag{1}$$

where P_0 and P_1 are the constant blade profile power and induced power in hovering status respectively; U_{tip} is the tip speed of the rotor blade; v_0 is the mean rotor induced velocity in hover; d_0 and s are the fuselage drag ratio and rotor solidity respectively; ρ denotes the air density in kg/m^3, and $G \triangleq \pi R^2$ denotes the rotor disc area in m^2 with R being the rotor radius.

2) RIS and Communication Model: As shown in Fig.1, there is a RIS deployed on the surface of the building to redirect the signals between UAV and GT, i.e. the UAV-GT link might be replaced by the two UAV-RIS and RIS-GT links. The RIS ensures the UAV-RIS and RIS-GT links being all in LoS connections. However, it is possible that the signal reflecting of the RIS cannot guarantee the LoS connection between UAV and RIS, like when the UAV-RIS link being closely blocked by the ground obstacles. In this letter, we will not consider such pessimistic situation and leave it to the further work. Following the same set up as in [10], the RIS has M reflecting elements to form a uniform linear array (ULA) and the location of the first element is denoted as $w_R = [x_R, y_R]^T$ in horizontal dimension and z_R in vertical dimension. To extend the work to support a uniform rectangular array (URA) at the RIS, which can be regarded as a specular reflector, the problem becomes to simultaneously deal with different groups of ULAs. In this case, the passive phase-shift of the RIS will have to work out the aliment of the phases that grouped as a rectangular array, i.e. matrix, instead of a liner array. Such extension therefore causes the passive-shift of the RIS and correlated joint optimization of UAV trajectory-task-cache to be a more complicated problem, and we will consider it in future work. To model the phase-shift of RIS, we assume $\theta_{in} \in [0, 2\pi), i \in M = \{1, ..., M\}$ to be the phase of the i-th reflecting element at time slot n, and $\Phi_n = \text{diag}\{e^{j\theta_{1n}}, e^{j\theta_{2n}}, ..., e^{j\theta_{Mn}}\}$ be the phase array of the M elements at time slot n, similar to [10]. Under this deployment, the channel gain of the UAV-RIS link at the n-th time slot is denoted by $g^{ur}_n \in \mathbb{C}^{M\times1}$,

$$g^{ur}_n = \frac{\sqrt{\xi}}{d^{ur}_n} \left[1, e^{-j\frac{2\pi}{\lambda}d\phi^{ur}_n}, ..., e^{-j\frac{2\pi}{\lambda}(M-1)d\phi^{ur}_n} \right]^T \tag{2}$$

where ξ is the path loss at the reference distance $D_0 = 1m$; $d^{ur}_n = \sqrt{(H - z_R)^2 + (q_n - w_R)^2}$; $\phi^{ur}_n = \frac{x_R - x_n}{d^{ur}_n}$ represents the cosine of the angle of arrival (AoA) of the signal at the n-th time slot; d is the antenna separation, and λ is the carrier wavelength. Meanwhile, the channel gain $g^{rg}_k \in \mathbb{C}^{M\times1}$ of the RIS to the k-th GT is given by

$$g^{rg}_k = \frac{\sqrt{\xi}}{d^{rg}_k} \left[1, e^{-j\frac{2\pi}{\lambda}d\phi^{rg}_k}, ..., e^{-j\frac{2\pi}{\lambda}(M-1)d\phi^{rg}_k} \right]^T \tag{3}$$

where $d^{rg}_k = \sqrt{z_R^2 + (w_R - w_k)^2}$; $\phi^{rg}_k = \frac{x_R - x_k}{d^{rg}_k}$ represents the cosine of the angle of departure (AoD) of the signal to the k-th GT. To this end, while the UAV-GT link being blocked, the channel gain achieved at GT k can be written as

$$g^{urg}_{kn} = c_{kn} \left(g^{rg}_k \cdot \Phi_n \cdot g^{ur}_n \right) \tag{4}$$

where $c_{kn} = \{0, 1\}$ denotes whether RIS will serve GT k or not at time slot n. One has $\sum_{k=1}^{K} c_{kn} = 1, \forall n$ denoting RIS only serve one GT at a time slot i.e. in TDMA mode. The more complicated OFDMA mode supporting multiple GTs served by the RIS at the same time slot, will be considered in future.

To evaluate the possibility that the direct UAV-GT link being blocked, we consider the air-to-ground channel model in urban environments [7], where the blocking probability between the UAV and the GT k at time slot n is given by

$$p_{kn} = 1 - \frac{1}{1 + a \exp\left(-b \left(\arctan\left(\frac{H}{d^h_k} \right) - a \right) \right)} \tag{5}$$

where $d^h_k = \sqrt{(q_n - w_k)^2}$; a and b are constant values depending on the environment. Then with $d^{ug}_k = \sqrt{H^2 + (q_n - w_k)^2}$, the average achievable channel gain g_{kn} and data rate r_{kn} of the k-th GT at time slot n are given by

$$g_{kn} = \underbrace{(1 - p_{kn}) \frac{\xi}{(d^{ug}_k)^2}}_{\text{UAV-GT}} + \underbrace{p_{kn} g^{urg}_{kn}}_{\text{UAV-RIS-GT}} \tag{6}$$

[*] In rest part of this letter, we may alternatively mention path segment as time slot, which are the same.

This article has been accepted for publication in a future issue of this journal, but has not been fully edited. Content may change prior to final publication. Citation information: DOI 10.1109/LWC.2021.3074990, IEEE Wireless Communications Letters

$$r_{kn} = B\log_2\left(1+\frac{p_k g_{kn}}{B\sigma^2}\right) \tag{7}$$

where p_k is the fixed transmit power of the UAV to GT k; B is the bandwidth; σ^2 is the noise variance.

3) Computation Model: According to task offloading, the latency of U_k is denoted as

$$L_k = (1-a_k)\frac{F_k}{f_k^l} + a_k\left(\frac{F_k}{f_k^o}+\frac{D_k}{r_k}\right),\ \forall k \tag{8}$$

where $r_k = \sum_{n=1}^{N} r_{kn}/N$ is the achieved average data rate of GT k; f_k^o is the UAV CPU cycles allocated to the task and f_k^l is the GT CPU cycles allocated to the task. $0 \le a_k \le 1$ is the indicator denoting the portion of the task offloaded from k-th GT to the UAV. One has $\sum_{k=1}^{K} a_k f_k^o \le C^o$, where C^o is the limited computation capacity. Due to the UAV-GT downlink normally has much higher data transferring rate, we ignore the downlink transmission time in (8).

The energy consumption of the UAV and GT on executing task U_k are formulated as

$$E_k^u = a_k E_k^o,\ \forall k \tag{9}$$

$$E_k^{gt} = a_k\frac{D_k}{r_k}p_k + (1-a_k)E_k^l,\ \forall k \tag{10}$$

where $E_k^o = \varphi(f_k^o)^{\vartheta-1}F_k$ and $E_k^l = \varphi(f_k^l)^{\vartheta-1}F_k$ are energy consumptions of the UAV and GT spent on task execution respectively; φ is the effective switched capacitance and $\vartheta \ge 1$ is the positive constant [7].

4) Cache Model: As it is known, one GT does not need to upload its task data, if its task already cached in the UAV [6] [7]. Therefore, (8), (9) and (10) can be re-formulated as

$$L_k^c = (1-x_k)L_k + x_k a_k\frac{F_k}{f_k^o},\ \forall k \tag{11}$$

$$E_k^c = (1-x_k)(\alpha E_k^{gt} + E_k^u) + x_k E_k^u,\ \forall k \tag{12}$$

where $0 \le x_k \le 1$ is the indicator denoting the portion of task k cached in the UAV. One has $\alpha > 0$ as the tradeoff between the energy consumptions of GT and UAV on serving task U_k. Assume $\sum_{k=1}^{K} x_k D_k \le C^c$ to indicate that the UAV having limited cache storage C^c.

B. Problem Formulation

Let $\mathbf{Q} = \{q_n, n \in \mathcal{N}\}$, $\mathbf{A} = \{a_k, k \in \mathcal{K}\}$, $\mathbf{X} = \{x_k, k \in \mathcal{K}\}$, $\mathbf{C} = \{c_{kn}, \forall k, \forall n\}$, and $\Phi = \{\Phi_n, n \in \mathcal{N}\}$, the optimization problem can be moded as

$$\mathcal{P}: \min_{\mathbf{Q},\,\mathbf{A},\,\mathbf{X},\,\mathbf{C},\Phi} \left(\sum_{n=1}^{N} e_n^{\text{uav}} + \beta\sum_{k=1}^{K} E_k^c\right) \tag{13}$$

$$\text{s.t.}\ \ 0 \le a_k \le 1,\ 0 \le x_k \le 1,\ \forall k; \tag{13.1}$$

$$\sum_{k=1}^{K} x_k D_k \le C^c; \tag{13.2}$$

$$\sum_{k=1}^{K} a_k f_k^o \le C^o; \tag{13.3}$$

$$T_k \ge L_k^c, \forall k; \tag{13.4}$$

$$q_1 = q_{N+1}; \tag{13.5}$$

$$\|q_{n+1} - q_n\| \le \min\{t_n V_{\max}^h, \Delta_{\max}^h\},\ \forall n; \tag{13.6}$$

$$c_{kn} = \{0,1\}, \sum_{k=1}^{K} c_{kn} = 1, \forall n, \forall k; \tag{13.7}$$

where $\mathcal{P}$ is to minimize the energy consumption of the UAV while satisfying the QoS requirement of tasks on latency; $\beta > 0$ is the tradeoff between the energy consumptions on UAV propulsion and serving GT tasks; (13.4) is the constraint on the service requirement of each task, i.e. task's latency being lower than its completion deadline; (13.5) $\sim$ (13.6) are the constraints on the trajectory of the rotary-wing UAV in horizontal dimension. Here, we assume the flight time of the UAV in each line segment is fixed to simplify the problem. Obviously, $\mathcal{P}$ is a non-convrx problem, which is difficult to be solved in its current form.

III. PROPOSED SOLUTION

According to SCA method, problem $\mathcal{P}$ can be decomposed into serval convex sub-problems. With the decomposition, we can design one iterative algorithm to solve those sub-problems in each steps in a loop, which will converge to a pre-defined accuracy and lead to the optimal results: $\{\mathbf{Q}, \mathbf{A}, \mathbf{X}, \mathbf{C}, \Phi\}^*$.

*A. Optimize Task Offloading and Cache Variables **A** and **X***

According to [7], with variables $\mathbf{Q}$, $\mathbf{C}$ and Φ fixed, we can directly solve following sub-problems $\mathcal{P}1$ and $\mathcal{P}2$ using CVX tool to obtain $\mathbf{A}$ and $\mathbf{X}$. The details on reforming $\mathcal{P}$ into $\mathcal{P}1$ and $\mathcal{P}2$ can be found in [7].

$$\mathcal{P}1: \min_{\mathbf{A}} \sum_{k=1}^{K} \hat{E}_k^c \quad \text{s.t.}\quad 0 \le a_k \le 1, \forall k;\ (13.3) \tag{14}$$

$$\mathcal{P}2: \max_{\mathbf{X}} \sum_{k=1}^{K} x_k a_k D_k \ \ \text{s.t.}\ \ 0 \le x_k \le 1, \forall k;\ (13.2) \tag{15}$$

where $\hat{E}_k^c = a_k E_k^o + \frac{\alpha H_k E_k^l}{a_k} + \alpha H_k\left(\frac{D_k}{r_k}p_k - E_k^l\right)$ is the re-formed E_k^c by introducing $H_k = \min\left\{\max\left\{\frac{T_k - \frac{F_k}{f_k^l}}{\frac{D_k}{r_k}+\frac{F_k}{f_k^o}-\frac{F_k}{f_k^l}}, 0\right\}, 1\right\}$ into (12); r_k is the average data rate calculated by (7), given $\mathbf{Q}$, $\mathbf{C}$ and Φ. $\mathcal{P}1$ and $\mathcal{P}2$ are to minimize the energy consumption on mobile computing while satisfying the task QoS on latency.

*B. Optimize Horizontal Trajectory **Q***

With variables $\mathbf{A}, \mathbf{X}, \mathbf{C}$, Φ fixed, $\mathcal{P}$ can be reformed into

$$\mathcal{P}3: \min_{\mathbf{Q}} \sum_{n=1}^{N} \hat{e}_n^{\text{uav}} \tag{16}$$

$$\text{s.t.}\ \ (13.5);\ (13.6); \sum_{n=1}^{N} r_{kn} \ge NR_k, \forall k; \tag{16.1}$$

$$\gamma_n^2 + \frac{(v_n^h)^2}{v_0^2} \ge \frac{1}{\gamma_n^2}; \tag{16.2}$$

This article has been accepted for publication in a future issue of this journal, but has not been fully edited. Content may change prior to final publication. Citation information: DOI 10.1109/LWC.2021.3074990, IEEE Wireless Communications Letters

where $\hat{e}_n^{\text{uav}} \triangleq t_n\left(P_0(1+\frac{3(v_n^h)^2}{U_{\text{tip}}^2})+\frac{1}{2}d_0\rho sG(v_n^h)^3+P_1\gamma_n\right)$, which is obtained by introducing slack variable $\gamma_n = \left(\sqrt{1+\frac{(v_n^h)^4}{4\upsilon_0^4}}-\frac{(v_n^h)^2}{2\upsilon_0^2}\right)^{\frac{1}{2}}$ into (1); $R_k = D_k/\left(\frac{T_k f_k^o - a_k x_k F_k}{a_k(1-x_k)f_k^o}-\frac{(1-a_k)F_k}{a_k f_k^l}-\frac{F_k}{f_k^o}\right)$ is constant and obtained by bringing (11) into constraint (13.4). We can find $\mathcal{P}3$ is still non-convex due to constraints (16.1) and (16.2).

To release (16.1), we only consider the LoS connection between UAV and GT, and apply the inequality transformation and the first-order Taylor expansion of the left side of (16.1) at local point q_n^l to obtain

$$\begin{aligned} r_{kn} &> B\log_2\left(1+\frac{(1-p_{kn})E}{(q_n-w_k)^2+H^2}\right) \\ &\geq B\log_2\left(1+\frac{(1-\tau p_{kn}^l)E}{(q_n-w_k)^2+H^2}\right) \\ &\geq J_{kn}^l\left((q_n-w_k)^2-(q_n^l-w_k)^2\right)+S_{kn}^l = r_{kn}^{bl} \end{aligned} \tag{17}$$

where $J_{kn}^l = \frac{-BE(1-\tau p_{kn}^l)}{\ln 2\left(((q_n^l-w_k)^2+H^2)^2+(1-\tau p_{kn}^l)E((q_n^l-w_k)^2+H^2)\right)}$; $S_{kn}^l = B\log_2(1+\frac{(1-\tau p_{kn}^l)E}{(q_n^l-w_k)^2+H^2})$; $E = \frac{p_k\xi}{B\sigma^2}$; p_{kn}^l is the probability of the N-LoS connection at local point q_n^l, and τ is the slack variable. We set $p_{kn} \leq \tau p_{kn}^l$ to denote the UAV-GT link getting LoS connection in a high enough probability. Then one has a new constraint as,

$$d_k^h = \sqrt{(q_n-w_k)^2} \leq \frac{H}{\tan\left(a-\frac{1}{b}\ln\frac{\tau p_{kn}^l}{a(1-\tau p_{kn}^l)}\right)} \tag{18}$$

Second, consider non-convex (16.2), at the given local points γ_n^l and $\hat{v}_n^h$ that are obtained following the last status of the UAV, we can apply the first-order Taylor expansion to γ_n to convert (16.2) to

$$\begin{aligned} &\gamma_n^4+\gamma_n^2\frac{(v_n^h)^2}{\upsilon_0^2} \geq X_n^{bl} = \\ &\left(4(\gamma_n^l)^3+2\gamma_n^l\frac{(\hat{v}_n^h)^2}{\upsilon_0^2}\right)\gamma_n-3(\gamma_n^l)^4-\frac{(\gamma_n^l\hat{v}_n^h)^2}{\upsilon_0^2} \geq 1 \end{aligned} \tag{19}$$

To this end, we simplify $\mathcal{P}3$ to

$$\mathcal{P}4: \min_{\mathbf{Q},\gamma_n} \sum_{n=1}^{N}\hat{e}_n^{\text{uav}} \tag{20}$$

$$\text{s.t. } (13.5);(13.6);(18);(19);\sum_{n=1}^{N} r_{kn}^{bl} \geq \epsilon N R_k; \tag{20.1}$$

where $0<\epsilon<1$ is the slack variable, and (20.1) denotes the UAV-GT link having to achieve certain level of data transmission rate coordinated by ϵ. $\mathcal{P}4$ is convex and can be directly solved by CVX tool.

C. Optimize phase-shift Φ and $\mathbf{C}$ of RIS

With variables **A, X, Q** fixed, $\mathcal{P}$ can be reformed as

$$\mathcal{P}5: \max_{\mathbf{C},\Phi}\min\nolimits_{\forall k}\left(\sum_{n=1}^{N} t_n r_{nk}\right) \text{ s.t. } (16.1);\ (13.7) \tag{21}$$

where $\mathcal{P}5$ is to optimize RIS to achieve the maximal minimum data transmission rate among all the GTs.

To make $\mathcal{P}5$ trackable, we convert (16.1) into a simpler form, considering passive phase-shift of RIS. In specific, assume RIS serves GT k at time slot n, i.e. $c_{kn}=1$, one has $g_k^{rg}\cdot\Phi_n\cdot g_n^{ur}$ in (4) written as

$$g_k^{rg}\cdot\Phi_n\cdot g_n^{ur} = \frac{\xi}{d_n^{ur}d_k^{rg}}\sum_{i=1}^{M} e^{j(\theta_{in}+\frac{2\pi}{\lambda}(i-1)d(\phi_k^{rg}-\phi_n^{ur}))} \tag{22}$$

To maximize the achievable rate of GT k, we can set

$$\theta_{in} = \frac{2\pi}{\lambda}(i-1)d(\phi_n^{ur}-\phi_k^{rg}) \tag{23}$$

which means the phase alignment of the signals at GT k is achieved given the trajectory of the UAV. Then, $g_k^{rg}\cdot\Phi_n\cdot g_n^{ur}$ can be rewritten as,

$$g_k^{rg}\cdot\Phi_n\cdot g_n^{ur} = \frac{M\xi}{d_n^{ur}d_k^{rg}} \tag{24}$$

If we bring (24) into (7), and only consider the N-LoS connection, the left side of (16.1) can be reformed as

$$R_{kn}^{'} = B\log_2(1+F) \geq B\log_2\left(1+\frac{p_{kn}p_k g_{kn}^{urg}}{B\sigma^2}\right) \tag{25}$$

where $R_{kn}^{'}$ is the upper bound of the data rate of the N-LoS connection, and $F = \frac{p_{kn}p_k M\xi}{B\sigma^2 d_n^{ur}d_k^{rg}}$. To this end, considering each GT, we can convert $\mathcal{P}5$ into K knapsack problems, each of which can be denoted as,

$$\mathcal{P}6: \max_{c_{kn},\forall n}\left(\sum_{n=1}^{N} t_n c_{kn} r_{kn}^{'}\right) \tag{26}$$

$$\text{s.t.}\quad (13.7),\ \sum_{n=1}^{N} c_{kn}R_{kn}^{'} \geq \delta N R_k \tag{26.1}$$

where δ is the slack variable. Obviously, we can solve $\mathcal{P}6$ to obtain $\mathbf{C}$ using liner program tool, and obtain Φ via (23).

D. Overall Algorithm Design

Based on the three steps in above sub-sections, the overall algorithm solving $\mathcal{P}$ can be designed as Algorithm 1. The algorithm can be proven to surely converge with an affordable computing complexity, following the similar analysis in [7].

Algorithm 1: Optimize trajectory-task-cache with RIS

```
Initialize the system to obtain: A^0, X^0, Q^0, C^0, Φ^0, i = 0;
repeat
    Obtain A^{i+1}, X^{i+1} soving P1 and P2, given Q^i, C^i, Φ^i;
    Obtain Q^{i+1} by soving P4, given Φ^i, C^i, A^{i+1}, X^{i+1};
    Obtain C^{i+1} by solving P6 and Φ^{i+1} via (23), given
        Q^{i+1}, A^{i+1}, X^{i+1}; i = i + 1;
until Converge to a prescribed accuracy;
Return A^{i+1}, X^{i+1}, Q^{i+1}, C^{i+1}, Φ^{i+1};
```

IV. Numerical Results

The proposed solution is validated through simulation using Matlab. We assume the UAV initially flying a circular

This article has been accepted for publication in a future issue of this journal, but has not been fully edited. Content may change prior to final publication. Citation information: DOI 10.1109/LWC.2021.3074990, IEEE Wireless Communications Letters

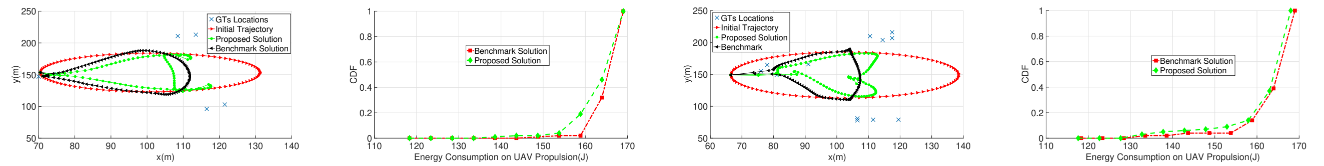

(a) UAV trajectories-6 GTs (b) UAV propulsion energy-6 GTs (c) UAV trajectories-12 GTs (d) UAV propulsion energy-12 GTs

Fig. 2. Performance comparisons on UAV trajectories and propulsion energy consumptions of different solutions.

trajectory as proposed in [13]. We set B: 2GHz; p_k: 5mW; σ : -169dBm/Hz; pathloss parameters a, b, η_{Los}, η_{NLos}, ξ, $\frac{d}{\lambda}$ to be: 0.961, 1.6, 1, 20, 3dB, 0.5 [7]; time slots t_n, N to be: 1s, 100; task computation and cache parameters: φ, ϑ, f_k^o, f_k^l, C^c, C^o to be: $10^{-9}, 3$, $200 \sim 400$MHz, $100 \sim 200$MHz, 1Gb, 1GHz. We set the RIS parameters: M, θ_{i1}, W_R, Z_R to be: 100, 0^o, $[0, 0]$, 20m respectively. And more settings on UAV and tasks can be found in the source code: https://github.com/HaiboMei/UAV-RIS-SCA.git.

We compare our proposed solution to the benchmark solution, which does not consider cache and dynamic offloading of the GT tasks. The benchmark solution thus always has to offload the GT tasks to the UAV. In addition, the benchmark solution does not consider RIS passive phase-shift neither. Meanwhile, we also compared the proposed solution to the one that does not consider RIS passive phase-shift. This is to testify how can RIS passive phase-shift help the data transmissions between UAV and GTs.

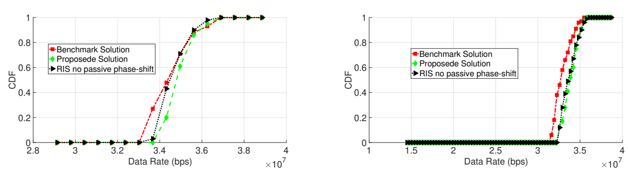

(a) UAV-GT date rate-6 GTs (b) UAV-GT date rate-12 GTs

Fig. 3. Performance comparisons on date transmission rate.

According to Fig.2(a) and Fig.2(c), we can easily find that the proposed solution controls the UAV to fly with energy-efficient routes, as compared to the benchmark solution in both two GT scenarios. Accordingly, the UAV propulsion energy consumptions in Cumulative Distribution Function(CDF) values are indicated to be lower led by the proposed solution in Fig.2(b) and Fig.2(d) (lower UAV propulsion energy consumption cumulatively distributed in left side of the x-axis). In Fig.3(a) and 3(b), the data rates of each UAV-GT link in each time slot are shown in CDF values. We can see that the proposed solution controls the UAV-GT pairs to have the highest data transmission rate (high UAV-GT data rates cumulatively distributed in right side of the x-axis). This justifies that the RIS passive phase-shift does help to improve the wireless transmission environment, while jointly working with UAV trajectory-task-cache optimization.

V. Conclusion

To improve the energy efficiency of the RIS-assisted UAV, this letter proposed a solution to jointly optimize the UAV trajectory, task offloading and cache with the design of RIS passive phase-shift. A SCA method is ultized to obtain a sub-optimal solution, which is proved to be effective. In future, we will consider RIS assisting multi-UAVs working as airborne MEC platform, and try to solve related optimization problems.

VI. Acknowledgement

This research was funded by Natural Science Foundation of China (Grant Nos. 61620106011, U1705263 and 61871076), and Quzhou Research Institute (Grant No. 2020D002).

References

[1] X. Hu, K. Wong, and K. Yang, “Wireless powered cooperation-assisted mobile edge computing,” *IEEE Transactions on Wireless Communications*, vol. 17, no. 4, pp. 2375–2388, 2018.

[2] S. Jeong, O. Simeone, and J. Kang, “Mobile cloud computing with a uav-mounted cloudlet: optimal bit allocation for communication and computation,” *IET Communications*, vol. 11, no. 7, pp. 969–974, 2017.

[3] Y. Du, K. Yang, K. Wang, G. Zhang, Y. Zhao, and D. Chen, “Joint resources and workflow scheduling in uav-enabled wirelessly-powered mec for iot systems,” *IEEE Transactions on Vehicular Technology*, vol. 68, no. 10, pp. 10 187–10 200, 2019.

[4] F. Zhou, Y. Wu, R. Q. Hu, and Y. Qian, “Computation rate maximization in uav-enabled wireless-powered mobile-edge computing systems,” *IEEE Journal on Selected Areas in Communications*, vol. 36, no. 9, pp. 1927–1941, 2018.

[5] Q. Hu, Y. Cai, G. Yu, Z. Qin, M. Zhao, and G. Y. Li, “Joint offloading and trajectory design for uav-enabled mobile edge computing systems,” *IEEE Internet of Things Journal*, vol. 6, no. 2, pp. 1879–1892, 2019.

[6] M. Chen, M. Mozaffari, W. Saad, C. Yin, M. Debbah, and C. S. Hong, “Caching in the sky: Proactive deployment of cache-enabled unmanned aerial vehicles for optimized quality-of-experience,” *IEEE Journal on Selected Areas in Communications*, vol. 35, no. 5, pp. 1046–1061, 2017.

[7] H. Mei, K. Wang, D. Zhou, and K. Yang, “Joint trajectory-task-cache optimization in uav-enabled mobile edge networks for cyber-physical system,” *IEEE Access*, vol. 7, pp. 156 476–156 488, 2019.

[8] M. Di Renzo, A. Zappone, M. Debbah, M. S. Alouini, C. Yuen, J. de Rosny, and S. Tretyakov, “Smart radio environments empowered by reconfigurable intelligent surfaces: How it works, state of research, and the road ahead,” *IEEE Journal on Selected Areas in Communications*, vol. 38, no. 11, pp. 2450–2525, 2020.

[9] C. Huang, A. Zappone, G. C. Alexandropoulos, M. Debbah, and C. Yuen, “Reconfigurable intelligent surfaces for energy efficiency in wireless communication,” *IEEE Transactions on Wireless Communications*, vol. 18, no. 8, pp. 4157–4170, 2019.

[10] S. Li, B. Duo, X. Yuan, Y. Liang, and M. Di Renzo, “Reconfigurable intelligent surface assisted uav communication: Joint trajectory design and passive beamforming,” *IEEE Wireless Communications Letters*, vol. 9, no. 5, pp. 716–720, 2020.

[11] H. Long, M. Chen, Z. Yang, B. Wang, X. Y. Z. Li, and M. Shikh-Bahaei, “Reflections in the sky: Joint trajectory and passive beamforming design for secure uav networks with reconfigurable intelligent surface,” 2020. [Online]. Available: https://arxiv.org/abs/2005.10559

[12] L.Wang, K. Wang, C. Pan, W. Xu, and N. Aslam, “Joint trajectory and passive beamforming design for intelligent reflecting surface-aided uav communications: A deep reinforcement learning approach,” 2020. [Online]. Available: https://arxiv.org/abs/2007.08380

[13] Q. Wu and R. Zhang, “Common throughput maximization in uav-enabled ofdma systems with delay consideration,” *IEEE Transactions on Communications*, vol. 66, no. 12, pp. 6614–6627, 2018.